

Interstellar extinction in the UV

M. J. Seaton *Department of Physics and Astronomy,
University College London, Gower Street, London WC1E 6BT*

Received 1979 April 9; in original form 1979 February 12

Summary. The UV interstellar extinction obtained from observations using the *OAO-2*, *Copernicus* and *TD-1* satellites, is fitted to simple analytical expressions in the variable $x = 1/\lambda$. The feature centred at $\lambda \approx 2200 \text{ \AA}$ can be fitted to a Lorentz profile; this result may be of physical significance.

1 Introduction

A mean UV interstellar extinction curve is required for the analysis of UV observations. We use the notation $X(x) = A_\lambda/E_{B-V}$ where; A_λ is the extinction in magnitudes; $E_{B-V} = A_B - A_V$ where A_B and A_V are the extinctions at the wavelengths of the *B* and *V* filters; and $x = 1/\lambda$ with λ in microns.

Observations made with the *OAO-2* satellite are reported by Bless & Savage (1972) for 19 stars and by Cashdollar & Code (1975) for 60 stars. A convenient tabulation of the *OAO-2* data, for λ out to 1100 \AA ($x = 9.09$), is given by Code *et al.* (1976, C76). *Copernicus* observations for four stars (York *et al.* 1973) are in good agreement with the *OAO-2* observations for x between 7.5 and 9.0, and extend out to $x = 10$. Observations with the *TD-1* satellite are reported by Nandy *et al.* (1975, N75) for about 100 stars and by Nandy *et al.* (1976, N76) for several hundred stars. The resolution with *OAO-2* is about 20 \AA at longer wavelengths and 10 \AA at shorter wavelengths. The *TD-1* resolution is about 30 \AA for $3.92 \leq x \leq 7.41$, and broad-band ($\sim 300 \text{ \AA}$) measurements are made at $x = 3.65$. The results of N76 are for photometric bands of width 100 \AA .

In the present paper we give analytical expressions for $X(x)$, obtained on fitting the observational data.

2 The ratio of total to selective extinction

For the mean ratio $R = A_V/E_{B-V}$, Seaton (1979) adopts $R = 3.17$ from a re-analysis of the *K* filter measurements of Smyth & Nandy (1978). Johnson (1977) recommends a mean value $R = 3.24$. We adopt $R = 3.20$.

The tabulations of $X(x)$ given by N75 and C76 extend into the optical region of ground-based observations. In this region the two tabulations are significantly different. Taking $x_U = 2.82$, $x_B = 2.31$ and $x_V = 1.83$ for the *U*, *B*, *V* filters we obtained $E_{U-V}/E_{B-V} = 1.61$

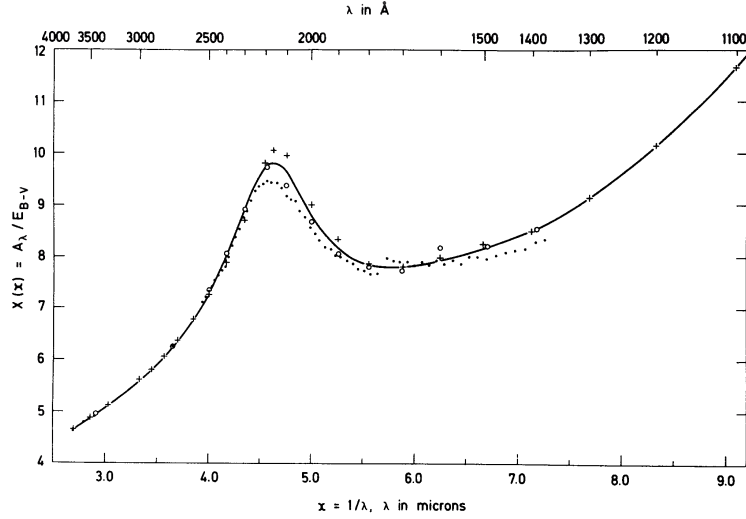


Figure 1. The UV extinction $X(x) = A_\lambda / E_{B-V}$ against $x = 1/\lambda$ with λ in microns. + OAO-2 data of C76 (Code *et al.* 1976); · TD-1 data of N75 (Nandy *et al.* 1975); ○ TD-1 data of N76 (Nandy *et al.* 1976). The full line curve is from the fits of Table 2.

from N75 and $E_{U-V}/E_{B-V} = 1.76$ from C76. Seaton (1979) notes that the tabulation of N75 is in close agreement with the best optical observations and obtains an independent check by considering the observed intensities of the H I and He II recombination lines in the planetary nebula NGC 7027. The values of $X(x)$ tabulated by N75 and N76 correspond to $R = 3.04$. We add 0.16 to these values to obtain results for $R = 3.20$.

The tabulation of $X(x)$ by C76 in the optical region gives $R = 3.11$, but in this region the C76 tabulation appears to be in less good agreement with optical observations. We therefore re-normalize the results of C76 by comparison with the results of N75, N76 in the near UV, $2.70 \leq x \leq 3.65$ (which includes the region of the *U* filter). In this near UV region there is a nearly constant difference between the results of C76 and N75, N76; $X(\text{C76}) - X(\text{N75 and N76}) = 0.20 \pm 0.02$. We therefore subtract 0.04 from the values of X tabulated by C76 to obtain results on the scale of N75 and N76 re-normalized to $R = 3.20$.

The adopted re-normalized observational results are shown on Fig. 1.

3 The 2200 Å feature

Examination of the results of Fig. 1 suggests that the feature at $\lambda \approx 2200 \text{ Å}$ ($x \approx 4.6$) may have very broad wings. It has been noted by Savage (1975) that in the region of the feature an excellent approximation is provided by a Lorentz function and a linear background. We therefore try fitting to

$$X(x) = a + bx + d / \{(x - x_0)^2 + \gamma^2\} \quad (1)$$

for x in some range $x_1 \leq x \leq x_N$, with the parameters a , b , d , x_0 and γ^2 determined by the method of least squares. Table 1 shows some results obtained by considering separately the different sets of data, C76, N75 and N76. The rms deviation is

$$\sigma = \left\{ (N - 5)^{-1} \sum_{i=1}^N [X_{\text{obs}}(x_i) - X_{\text{fit}}(x_i)]^2 \right\}^{1/2} \quad (2)$$

where N is the number of terms in the summation and 5 the number of adjustable parameters in the fit. The values of σ are within the errors of observation, and a good deal smaller than the differences between the three sets of observations.

Table 1. Least-squares fits of the individual sets of data, using equation (1).

Data set	Fit for $x_1 \leq x \leq x_N$		Parameters of fit						
	x_1	x_N	a	b	d	x_0	γ^2	N	σ
C76	3.45	5.88	2.50	0.813	0.967	4.64	0.261	14	0.07
N75	2.70	6.64	2.19	0.809	1.276	4.57	0.364	47	0.07
N76	2.91	5.56	2.03	0.887	1.064	4.56	0.299	12	0.05

There are significant differences between the *OAO-2* and *TD-1* results for the parameters x_0 and γ^2 , determining the position and width of the feature. Since there are no obvious reasons for preferring the *OAO-2* or the *TD-1* data, we adopt mean values from C76 and N76, to obtain $x_0 = 4.60$, $\gamma^2 = 0.280$.

4 The final fits

In order to obtain what are judged to be best fits for all of the data, we consider three ranges of x . With the adopted values of x_0 and γ^2 , we first choose a , b and d in equation (1) to give a best fit of the C76 and N76 data in the range $3.65 \leq x \leq 7.14$. Then, with the same value of the parameter d (which fixes the strength of the 2200 Å feature), we re-determine a and b (which fix the background) for the range $2.70 \leq x \leq 3.65$. Finally, for $7.14 \leq x \leq 9.09$ we fit to a quadratic,

$$X(x) = a + bx + cx^2. \quad (3)$$

The results obtained are given in Table 2 and shown as a full line curve in Fig. 1. Due to the use of smoothing and averaging, the fitted curve may be more accurate than any of the individual observational points. The agreement between the different observations is particularly good in the near UV, out to $x = 4.0$. The largest discrepancies are in the region of the maximum of the 2200 Å feature. Although there are few points plotted on Fig. 1 for the largest values of x , $x \geq 7.14$, the accuracy of the *OAO-2* data is confirmed by the *Copernicus* data, which also show that the fitted curve for $7.14 \leq x \leq 9.09$ can be used out to $x = 10.0$.

For ease of reference we give, in Table 3, values of $X(x)$ for $1.0 \leq x \leq 2.7$ from N75, re-normalized to $R = 3.20$.

Table 2. Adopted fits.

Range of x	Expression for $X(x)$
$2.70 \leq x \leq 3.65$	$1.56 + 1.048x + 1.01/\{(x - 4.60)^2 + 0.280\}$
$3.65 \leq x \leq 7.14$	$2.29 + 0.848x + 1.01/\{(x - 4.60)^2 + 0.280\}$
$7.14 \leq x \leq 10$	$16.17 - 3.20x + 0.2975x^2$

Table 3. Values of $X(x) = A_\lambda/E_{B-V}$ for $1.0 \leq x \leq 2.7$, from Nandy *et al.* (1975), re-normalized to $R = 3.20$.

x	$X(x)$	x	$X(x)$	x	$X(x)$
1.0	1.36	1.6	2.66	2.2	3.96
1.1	1.44	1.7	2.88	2.3	4.15
1.2	1.84	1.8	3.14	2.4	4.26
1.3	2.04	1.9	3.36	2.5	4.40
1.4	2.24	2.0	3.56	2.6	4.52
1.5	2.44	2.1	3.77	2.7	4.64

For the analysis of nebular spectra it is customary to use an extinction function $f(\lambda)$ such that the extinction is

$$10^{-C[1+f(\lambda)]} \quad (4)$$

where $f(\lambda)$ is such that $f(\lambda_\beta) = 0$, $\lambda_\beta = 0.4861 \mu\text{m}$ being the wavelength of the $\text{H}\beta$ line; C is then the logarithmic extinction at $\text{H}\beta$. We obtain

$$f(\lambda) = \frac{X(\lambda)}{X_\beta} - 1 \quad (5)$$

where $X_\beta = X(1/\lambda_\beta) = 3.68$ and $c = 0.4 X_\beta E_{B-V} = 1.47 E_{B-V}$.

5 Discussion of the 2200 Å feature

We do not have any unique way of separating the 'feature' from the 'back-ground'. Hence the fit of equation (1) may have no physical significance. However, a Lorentz profile is interesting in that it can be produced by simple physical processes. Interpreted as a transition probability Γ , the width $\gamma = \sqrt{(0.280)}$ corresponds to $\Gamma = 1.99 \times 10^{15} \text{s}^{-1}$. Lorentz profiles can be given by pressure broadening (which can be ruled out because the pressures are too low and the width is everywhere nearly the same), by radiation damping (which would require an oscillator strength $f \approx 1.4 \times 10^6$ and hence be possible only for a collective excitation of a system containing at least 1.4×10^6 electrons) or by auto-ionization or auto-dissociation. Auto-dissociation has been discussed previously (see, e.g. N75) and dismissed on the grounds that it will destroy the particle concerned, which cannot be replenished sufficiently rapidly. Auto-ionization of a molecule will give a molecular ion which may subsequently undergo dissociative recombination. Possibly these difficulties could be overcome by considering a molecule on the surface of a grain.

Acknowledgments

I thank Dr K. Nandy and Professor R. Wilson for discussions about this work, and a referee for helpful comments.

References

- Bless, R. C. & Savage, B. D., 1972. *Astrophys. J.*, **171**, 293.
- Cashdollar, K. & Code, A. D., 1975. Quoted by Code *et al.* 1976.
- Code, A. D., Davis, J., Bless, R. C. & Hanbury Brown, R., 1976. *Astrophys. J.*, **203**, 417.
- Johnson, H. L., 1977. *Rev. Mex. Astr. Astrofis.*, **2**, 219.
- Nandy, K., Thompson, G. I., Jamar, C., Monfils, A. & Wilson, R., 1975. *Astr. Astrophys.*, **44**, 195.
- Nandy, K., Thompson, G. I., Jamar, C., Monfils, A. & Wilson, R., 1976. *Astr. Astrophys.*, **51**, 63.
- Savage, B. D., 1975. *Astrophys. J.*, **199**, 92.
- Seaton, M. J., 1979. *Mon. Not. R. astr. Soc.*, **187**, 785.
- Smyth, M. J. & Nandy, K., 1978. *Mon. Not. R. astr. Soc.*, **183**, 215.
- York, D. G., Drake, J. F., Jenkins, E. B., Morton, D. C., Rogerson, J. B. & Spitzer, L., 1973. *Astrophys. J.*, **182**, L1.